*31st EPS Conference on Plasma Phys. London, 28 June - 2 July 2004 ECA Vol.**28G**, P-4.134 (2004)*

L-H transition at Low Densities in ASDEX Upgrade

S.V. Lebedev[1], F. Ryter[2], H-U. Fahrbach[2], V.E. Golant[1], W. Suttrop[2], H. Zohm[2]
and ASDEX Upgrade Team[2]

[1] *Ioffe Physico-Technical Institute, St. Petersburg, Russia, sergei.lebedev@mail.ioffe.ru*
[2] *Max-Planck-Institut für Plasmaphysik, EURATOM Association, Garching, Germany*

An increase of the *LH* transition power threshold towards low density has been observed in many experiments [1,2,3,4]. Various mechanisms were suggested to explain this behaviour: mode locking on DIII-D [2], electron-ion decoupling on ASDEX Upgrade [3], destabilization of peeling modes on COMPASS-C [4]. The actual physics reason has not been identified yet. This topic is being addressed in the recent study performed on ASDEX Upgrade.

The *LH* transition at average densities in the range of $0.188\text{-}0.35\cdot10^{20}$ m^{-3} was studied in ASDEX Upgrade in discharges with various heating schemes: ECRH (up to 1.9 MW), ICRH (up to 2.8 MW), NBI (up to 2.5 MW), ohmic (up to 0.92 MW). Combined scenarios: ECRH+ICRH, ECRH+NBI, ICRH+NBI were included in the data set as well. In the experiments the net heating power inside separatrix P_{net} (defined by total input power with subtracted power of neutral beam direct losses and derivative of stored energy) was varied from 0.36 to 2.6 MW. Radiation losses are neglected in this consideration. Plasma current I_p and toroidal field B_t were in the ranges of 0.54-1.07 MA and 1.3-2.7 T, respectively. All shots were performed in a single null divertor configuration with elongation $k \approx 1.6$ and triangularity δ_{up} varied from -0.072 to 0.306 (note, here δ_{up} is the triangularity calculated for the upper point of the plasma cross-section. X-point position at the bottom of cross-section was fixed at $\delta_{lo} \approx 0.3$). The ion *gradB* drift was directed towards the X-point.

The dataset considered contains 58 time slices preceding the *LH* transitions and 29 time slices without *LH* transitions, see fig.1. Later definition: "without *LH* transition" means that transition does not occur for at least 0.2 *s* (several energy confinement times) after chosen time slice. At densities higher than $0.325\cdot10^{20}$ m^{-3} (region I on fig.1) the *LH* transition threshold power is in agreement with the scaling describing ASDEX Upgrade data [5]: $P_{thr} = 1.98\ \bar{n}^{0.79} B_t^{0.56}$, here P_{thr}, $\bar{n}$ and B_t are expressed in MW, 10^{20} m^{-3} and T, correspondingly. At densities below $0.21\cdot10^{20}$ m^{-3}, no transition was observed for the applied power P_{net} up to 2.06 MW, see region III on fig.1. In the density range $0.21\text{-}0.325\cdot10^{20}$ m^{-3} a very large scatter in the threshold power has been found. The scatter might appear if other parameters than density and toroidal field influence the threshold power or if the dependencies of P_{thr} on $\bar{n}$ and B_t differ from the above scaling. The effects of B_t, I_p, δ_{up} and heating method on the threshold power in this density range were analyzed.

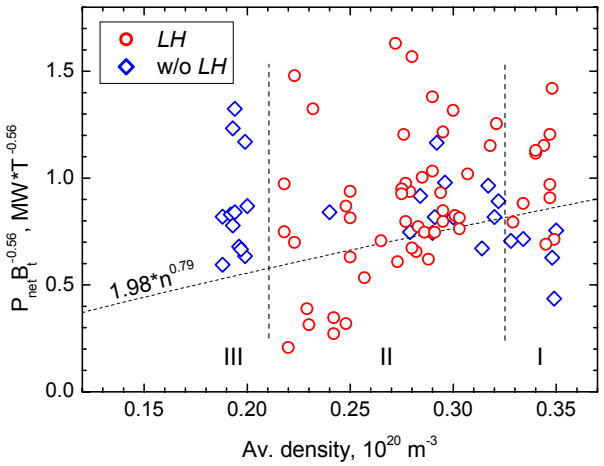

Fig.1. Net heating power inside separatrix normalized by $B_t^{0.56}$ as a function of average density, red circles – shots with LH transitions, blue diamonds – shots without LH transitions.

Features of the LH transition at low density

The *LH* transitions at low density (in the range of 0.21-0.3·10^{20} m^{-3}) differ from higher density transitions ($\bar{n}$ >0.3·10^{20} m^{-3}). The low density transitions are slow, dithering occurs frequently and the transitions have often two steps. The transitions at low density (or the first step when 2 steps are observed) are characterized by increases in the edge T_e and stored energy, but changes in the particle confinement are moderate, as could be estimated from $\bar{n}$ derivative. One example of the transition at density 0.22·10^{20} m^{-3} in the NBI heated shot (#17503) is presented on fig.2. The slack *LH* transition occurs at 5.17 s. Notice the weak effect on density increment at the time of the transition. For comparison the transition in the NBI heated shot #15155 at $\bar{n}$ =0.303·10^{20} m^{-3} is shown on fig.3. Although the NBI power is smaller in this case, the transition (t =1.67 s) is quite different: pronounced drop in the D-alpha emission, clear increases in the average density, stored energy and edge T_e.

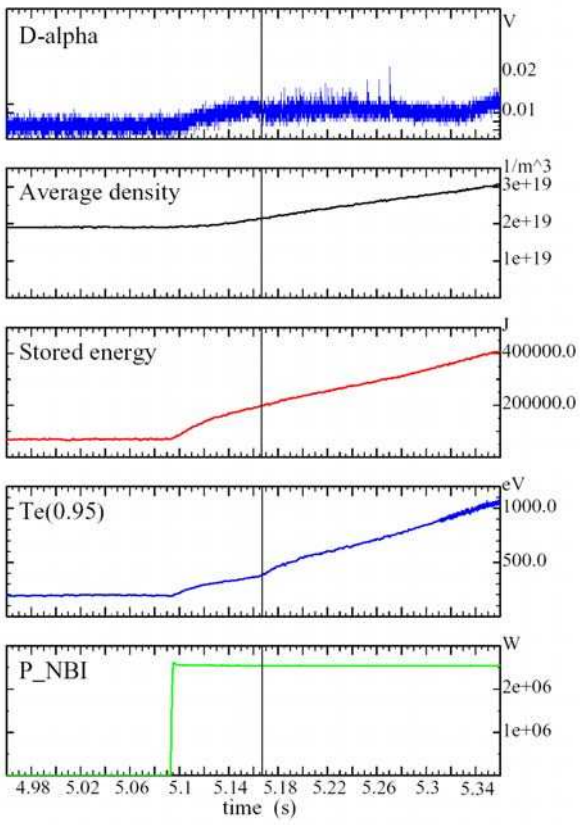

Fig.2. LH transition in the NBI heated shot #17503 at low density. Windows from top to bottom: D-alpha in the divertor, average density, stored energy, electron temperature at ρ_pol=0.95, NBI power.

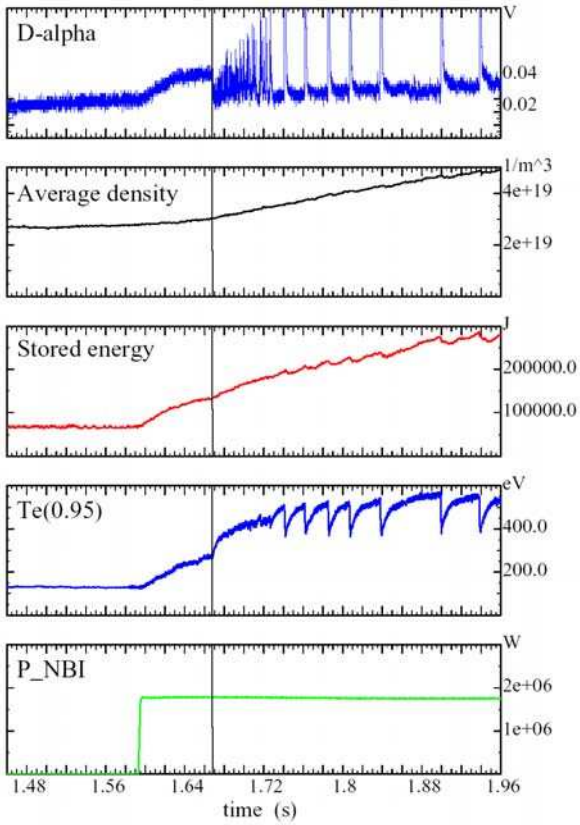

Fig.3. LH transition in the NBI heated shot #15155 at "normal" density. Windows (top to bottom): D-alpha in the divertor, average density, stored energy, electron temperature at ρ_pol=0.95, NBI power.

No essential difference was observed between ECRH and NBI assisted transitions at low densities. That suggests a common nature of transition physics, in spite of difference in the threshold behaviour. (See last section for analysis of difference in the *LH* transition threshold behaviour in ECRH and NBI heated shots.)

Effects of B_t, I_p, δ_{up} on threshold power

Possible deviation of *LH* transition threshold power from the above mentioned scaling expression P_{thr}=1.98$\bar{n}^{0.79}B_t^{0.56}$ [5] in the density range of 0.21-0.325·10^{20} m^{-3} (region II on fig.1) was analyzed statistically. In particular, dependencies of the threshold on toroidal

field and plasma were explored. The dataset containing 47 time slices preceding the *LH* transition with various heating schemes (NBI, ECRH, ICRH, NBI+ECRH, ICRH+ECRH) was fitted by expression $P_{thr} = A\,\bar{n}^{0.79} I_p^{b1} B_t^{b2}$ (note the density dependency was kept $\bar{n}^{0.79}$ from [5]). By regression the following values were obtained: $A = 3.16^{+1.49}_{-1.01}$, $b1 = 0.79 \pm 0.36$ and $b2 = 0.36 \pm 0.45$. The results indicate tendency of increase in the threshold with I_p, although reliability of the conclusion is not very high, since error of $b1$ is 46% of its value. Tendency of increase of P_{thr} with B_t is in line with scaling [5], but error in B_t-exponent even larger than its magnitude.

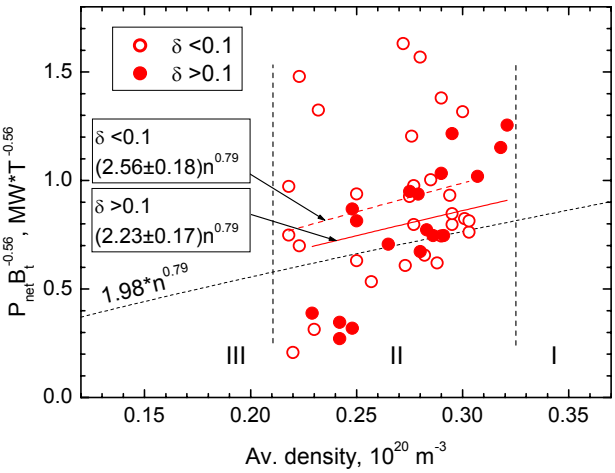

Fig.4. Comparison of two fits for LH transition power obtained for subsets of data with lower δ_{up} – open symbols and higher δ_{up} – solid symbols.

In order to derive the effect of triangularity δ_{up} on *LH* transition threshold the dataset was divided into two parts. The first part contained 29 time slices in shots with δ_{up} <0.1 and other one contained 18 time slices in shots with δ_{up} >0.1. Assuming the validity of $\bar{n}^{0.79} B_t^{0.56}$ the two fits were obtained. Comparison of these fits indicates some 15% decrease in the threshold power at δ_{up} >0.1, see fig.4. It should be noticed that the above finding is in contradiction with the earlier observations in ASDEX Upgrade [6], where some increase in the P_{thr} with δ have been found in the density range $0.28 < \bar{n}\,[10^{20}\mathrm{m}^{-3}] < 0.9$ and $\delta > 0.1$.

The high values of relative errors of I_p and B_t exponents and moderate difference between fits with δ_{up} <0.1 and δ_{up} >0.1 indicate that considered dataset is not conclusive for derivation of P_{thr} dependencies on I_p, B_t and δ in the range of $0.21 < \bar{n} < 0.325 \cdot 10^{20}$ m^{-3}. In the next section, we will explore effect of local parameters (edge T_e) on P_{thr}.

Effect of heating method on threshold power

At low densities the electron-ion energy exchange is low such that the electron and ion temperature are relatively directly linked to the respective heat fluxes and can therefore differ significantly. Under these conditions the dominant heating of either component may facilitate or hamper the *LH* transition. From the available dataset the cases with either dominant electron or dominant ion heating can be separated. The separation yields 18 time slices with ECR and 39 time slices with NBI. ECRH provides direct dominant electron heating and weak ion heating through e-i energy exchange only. The NBI provides more ion heating, although a fraction of the power goes to electron component due to slowing down of beam ions by thermal electrons. Figs.5&6 present the subsets of ECRH and NBI shots.

In the density range considered there are not many ECRH assisted *LH* transitions: only three shots in the dataset. In the low density region III ($\bar{n} < 0.21 \cdot 10^{20}$ m^{-3}) no transition was observed with ECRH alone using the available power P_{net} up to 2.06 MW, see fig.5. In the NBI scenario the *LH* transition could be observed down to $0.22 \cdot 10^{20}$ m^{-3}, fig.6. Lower densities are not accessible with NBI, since the density increases as soon as heating is turned

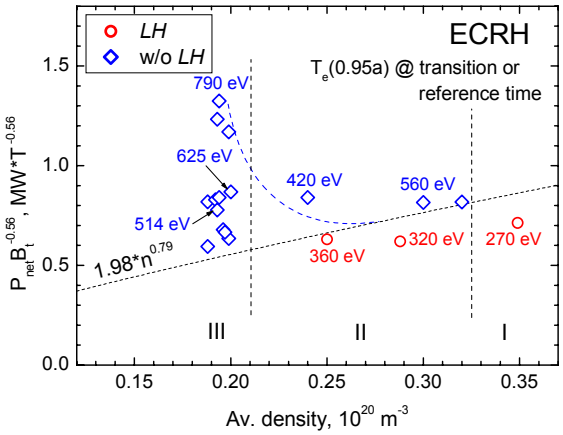

Fig.5. P_{thr} *increase in the ECRH low* $\overline{n}$ *shots. No LH transition occurs at* $\overline{n}$ *<0.245·10*^{20} *m*$^{-3}$.

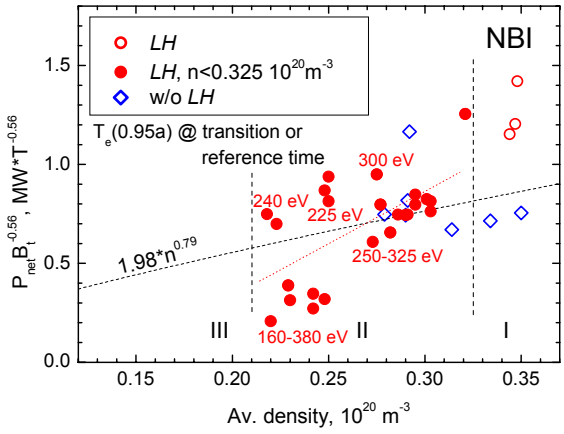

Fig.6. P_{thr} *decrease in the NBI shots. Doted line is the linear fit for the solid circles (*$\overline{n}$ *<0.325·10*^{20}*m*$^{-3}$*)*

on. P_{net}, at which the transition occurs, were as low as 0.33 MW at P_{NBI}=2.5 MW and 1.14 MW at P_{NBI}=1.32 MW (The difference in the P_{net} is due to the high dW/dt in the first case). With the NBI heating the necessary *LH* transition power at low density appears to decrease below the scaling P_{thr}=1.98 $\overline{n}^{0.79} B_t^{0.56}$. However, P_{thr} in this case has large uncertainty (Linear fit (see fig.6) reads $P_{thr}/B_t^{0.56}$=(-0.72±0.36)+(5.29±1.35) $\overline{n}$). Note that at large dW/dt, P_{net} may underestimate the edge heating if the source is finite at the edge.

Clear increase in the threshold power with ECRH and some decrease with NBI at low density suggest effect of heating scheme on P_{thr}. It is interesting to note that the edge electron temperature is quite different in the time slices preceding the *LH* transition and in the time slices without subsequent transition. On fig.5 the T_e measured in the equatorial plane at the flux surface ρ_{pol}=0.95 is given. Higher edge T_e values are observed in the shots without transition. Lower values for the edge T_e are found in the NBI shots with *LH* transition. In the shots presented on fig.6 the $T_e(0.95)$ were in the range of 0.16 to 0.38 keV.

These observations may be interpreted in two ways. The first possibility is to assume that high edge T_e, or its gradient, hampers the *LH* transition. As one expects low edge T_i values at low density with ECRH, the second possibility is that the edge T_i, or its gradient, plays a key role, as suggested by JET results [7]. The latter hypothesis is expected to be investigated soon using the new edge T_i diagnostic at ASDEX Upgrade [8].

Acknowledgements. S.V. Lebedev and V.E. Golant are grateful to the Alexander-von-Humboldt Foundation and MPI Garching for the financial support provided for this study; they acknowledge scientific encouragement and helpful discussions held in MPI Garching.

References

1. F. Wagner, et al, PRL, 49(1982), 1408
2. K. Burrell, et al, PRL, 59(1987), 1432
3. F. Ryter, et al, PPCF, 36(1994), A99
4. S. Fielding, et al, IAEA, Seville, 1994, v.II, 29
5. F. Ryter, et al, PPCF, 44 (2002), A415
6. R. New, et al, Nuclear Fusion, 43(2003), 1191
7. Y. Andrew, et al, PPCF, 46(2004), 337
8. M. Reich, et al, PPCF, 46(2004), 797; also this EPS Conference Proceedings